# UNDRAINED SOIL BEHAVIOUR

This document verifies that the undrained analysis of partially saturated soil is correctly implemented in PLAXIS. Bishop's effective stress (Bishop & Blight, 1963) is used in PLAXIS to handle unsaturated soil conditions. In undrained analysis, excess water pore pressures are generated based on the water bulk modulus, the value of which depends on the Soil Water Characteristic Curve (SWCC), i.e. the relationship between the degree of saturation and the applied suction. It is attempted to show how the SWCC affects the undrained behaviour of soil.

Used version:

- PLAXIS 2D - Version 2018.0
- PLAXIS 3D - Version 2018.0

**Geometry:** The model geometry in PLAXIS 2D is presented in Figure 1. A plane-strain model with 15-noded elements is used. The phreatic level is initially set at 1 m. All groundwater flow boundaries except for the top boundary are set to *Closed* (impervious). The top model boundary is set to *Open* (seepage). A vertical *Line load* is placed at the top boundary, with magnitude equal to 10 kN/m/m.

In PLAXIS 3D, the same model as described above is used, extended by 1 m in y-direction. The same groundwater flow boundary conditions are adopted. Additionally, both groundwater flow boundaries in y-direction are set to be *Closed*. A vertical *Surface load* is placed at the top boundary, with magnitude equal to 10 kN/m$^2$. Figure 2 illustrates the model geometry in PLAXIS 3D.

The position of the phreatic level leads to unsaturated starting flow conditions at the top half of the model. Suction equals 10 kPa at the top of the model and 0 kPa below the phreatic level. Three different cases of the SWCC are studied:

- Case 1: fully saturated material
- Case 2: partially saturated *coarse* material
- Case 3: partially saturated *fine* material

As presented in Figures 1 and 2, all three cases are studied together in one model for both PLAXIS 2D and PLAXIS 3D.

> **Hint:** To simulate all three cases in one model, three separate soil columns have to be created. Special treatment is needed for the groundwater flow boundary conditions, which should be *Closed* for every boundary except for the top. Additionally, *Line/Surface displacements* have to be used to fix normally the side boundaries of each soil column.

**Materials:** The soil is modeled as *Undrained (A)*, *Linear elastic*. The adopted mechanical material parameters are the same for cases 1 to 3:

| | | | | |
|---|---|---|---|---|
| Soil: | Linear elastic | Undrained (A) | $\gamma_{unsat}$ = 20 kN/m$^3$ | $\gamma_{sat}$ = 20 kN/m$^3$ |
| | $E'$ = 1000 kN/m$^2$ | $\nu'$ = 0.0 | $e_{init}$ = 0.50 | |

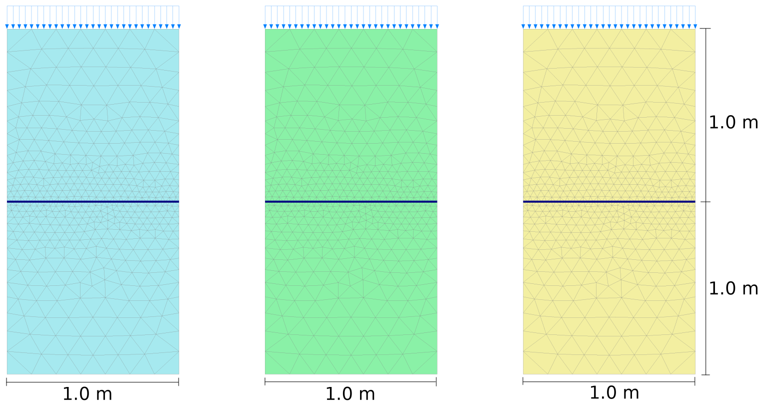


Figure 1 Problem geometry and generated mesh (PLAXIS 2D)

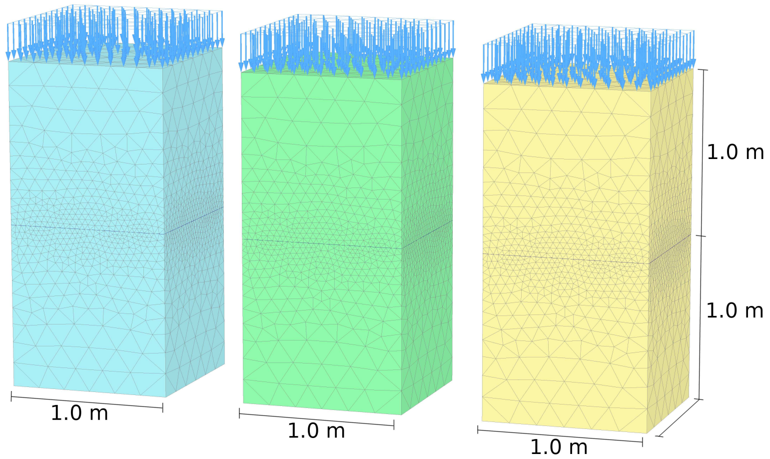


Figure 2 Problem geometry and generated mesh (PLAXIS 3D)

Regarding the hydraulic material properties, Table 1 presents the selected hydraulic model and the values of the corresponding flow parameters for cases 1 to 3. The *Van Genuchten* hydraulic model is used to model the unsaturated flow conditions in cases 2 and 3. The Van Genuchten parameters used for the coarse and fine topsoil material type may be found in Section 6.1.3 of the Reference Manual.

Table 1 Hydraulic material parameters

| Parameter | Symbol | Unit | Case 1 | Case 2 | Case 3 |
|---|---|---|---|---|---|
| Data set | - | - | User-defined | Hypres | Hypres |
| Model | - | - | Saturated | Van Genuchten | Van Genuchten |
| Soil type | - | - | - | Topsoil (coarse) | Topsoil (fine) |
| Saturated degree of saturation | $S_{sat}$ | - | 1.0 | 1.0 | 1.0 |
| Residual degree of saturation | $S_{res}$ | - | - | 0.062 | 0.019 |
| Permeability of saturated soil | $k$ | m/day | 1.0 | 1.0 | 1.0 |

Based on van Genuchten (1980) and the selected hydraulic material parameters presented in Table 1, the degree of saturation $S$ is plot against suction (SWCC) in Figure 3.

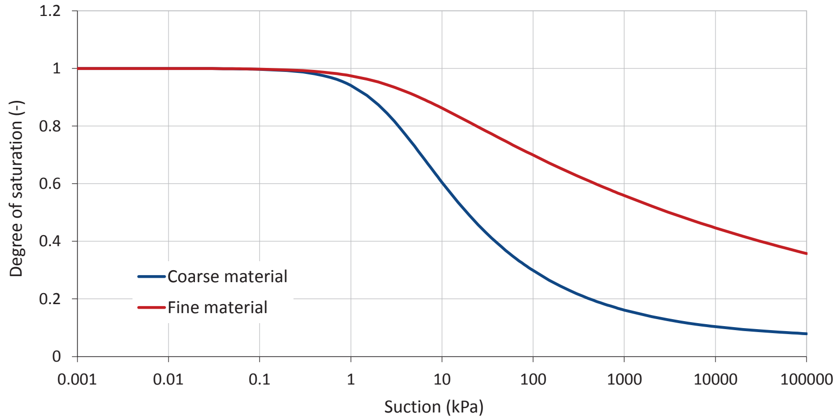


Figure 3 Degree of saturation $S$ versus suction

For suction equal to 10 kPa (top model boundary), the degree of saturation for the coarse material is $S_{coarse}$ = 0.6049, while for the fine material is $S_{fine}$ = 0.8623.

**Meshing:** In PLAXIS 2D, the *Very fine* option is selected for the *Element distribution*, while in PLAXIS 3D, the *Fine* option is used. The geometric line/surface representing the phreatic level is refined with a *Coarseness factor* of 0.2 in PLAXIS 2D and PLAXIS 3D as well. The generated mesh is illustrated in Figures 1 and 2.

**Calculations:** The calculations are performed using the *K0 procedure* calculation type in the Initial phase. The groundwater flow boundary conditions are adjusted as described above and the *Ignore suction* option is deactivated. A *Plastic* calculation is performed in Phase 1 and the *Line/Surface* loads are activated. The *Reset displacements to zero* option is selected, while the *Ignore suction* option remains deactivated.

**Output:** Figures 4 and 5 depict the vertical strains after the plastic analysis (Phase 1). Figures 6 and 7 illustrate the excess pore pressures after the plastic analysis (Phase 1). Figures 8 and 9 present the vertical effective stresses after the plastic analysis (Phase 1).

**Verification:** The equivalent bulk modulus of water for Plastic (undrained) analysis of an undrained material type in fully saturated soil conditions (S = 1) is:

$$\frac{K_w^{sat}}{n} = \frac{2G}{3}\left(\frac{1+\nu_u}{1-2\nu_u} - \frac{1+\nu'}{1-2\nu'}\right) \tag{1}$$

in which $n$ is the porosity of the soil and $\nu_u$ is the undrained Poisson's ratio, assumed equal to 0.495 for fully saturated conditions. Based on the input parameters used in the present example, $K_w^{sat}$ = 49500 kPa.

The bulk modulus of water $K_w^{unsat}$ for Plastic (undrained) analysis of an undrained material type in unsaturated soil conditions ($S < 1$) is a function of the degree of saturation $S$, formulated as (after Bishop & Eldin (1950), Fredlund & Rahardjo (1993) and

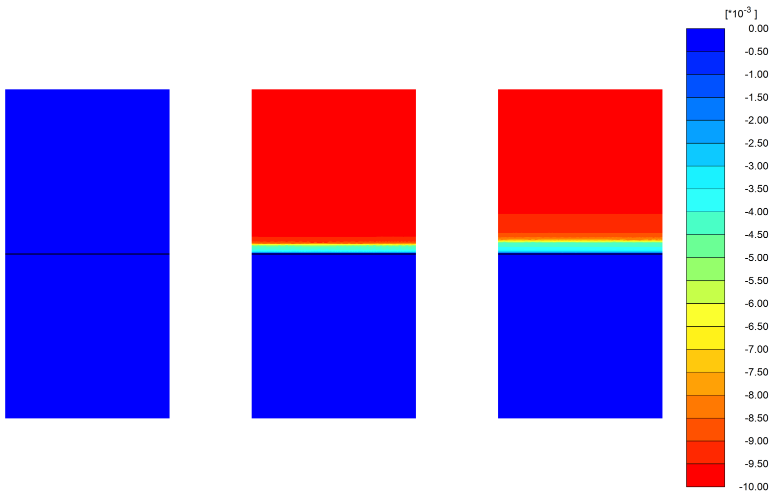


Figure 4 Vertical strains after the plastic analysis (Phase 1) in PLAXIS 2D

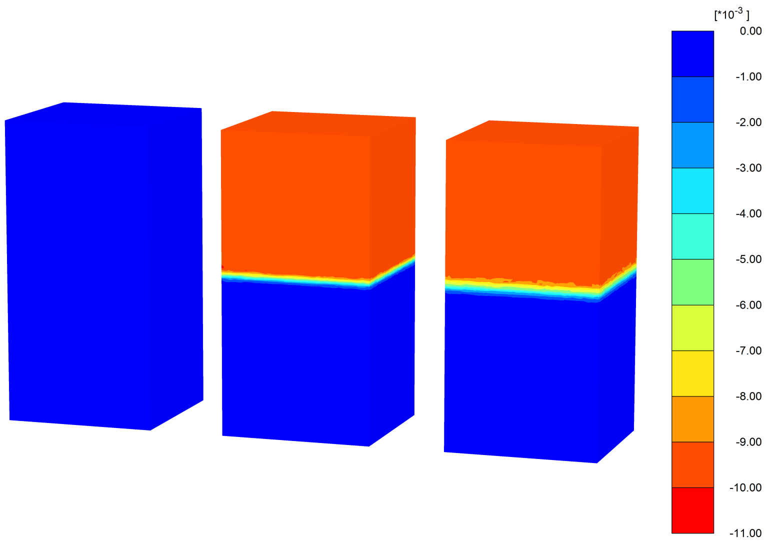


Figure 5 Vertical strains after the plastic analysis (Phase 1) in PLAXIS 3D

Verruijt (2001)):

$$K_w^{unsat} = \frac{K_w^{sat} K_{air}}{S K_{air} + (1 - S) K_w^{sat}} \tag{2}$$

in which $K_{air}$ is the bulk modulus of air. Assuming that air pore pressure $p_{air}$ equals zero, an artificial small value of 1 kPa is assigned to $K_{air}$. Based on the input parameters used in the present example, the unsaturated equivalent bulk modulus of water at the top of the model (suction equal to 10 kPa) is $K_w^{unsat,coarse}$ = 2.53 kPa and $K_w^{unsat,fine}$ = 7.26 kPa.

To estimate the vertical strain $\epsilon_v$ caused by the external stress of 10 kPa applied at the

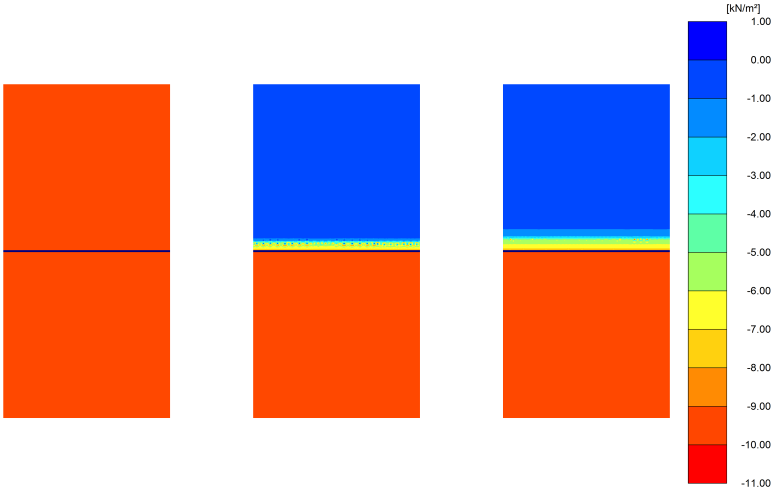


Figure 6  Excess pore pressures after the plastic analysis (Phase 1) in PLAXIS 2D

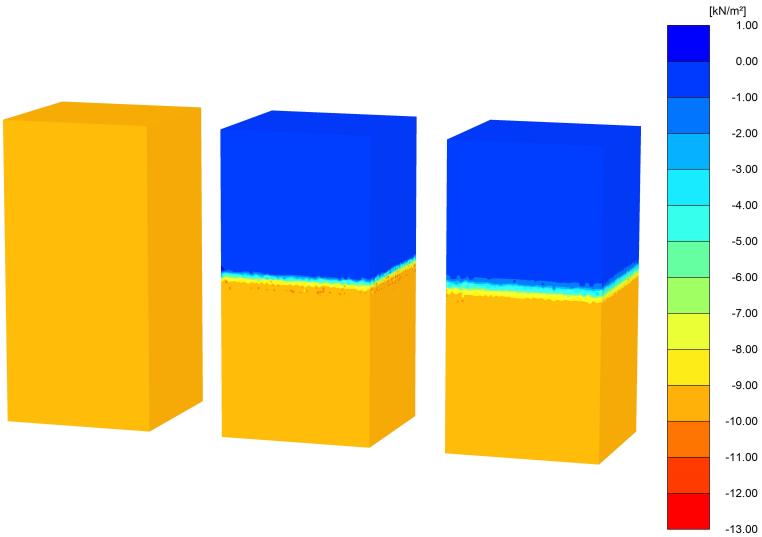


Figure 7  Excess pore pressures after the plastic analysis (Phase 1) in PLAXIS 3D

top of the model, the undrained oedometer modulus $E_{oed,u}$ is calculated as:

$$E^{sat}_{oed,u} = \frac{(1-\nu_u)E_u}{(1-2\nu_u)(1+\nu_u)} \quad \text{(for S = 1)} \tag{3}$$

$$E^{unsat}_{oed,u} = K' + \frac{4}{3}G + \frac{K^{unsat}_w}{n} \quad \text{(for S < 1)} \tag{4}$$

in which,

$$E_u = 2G(1+\nu_u) \tag{5}$$

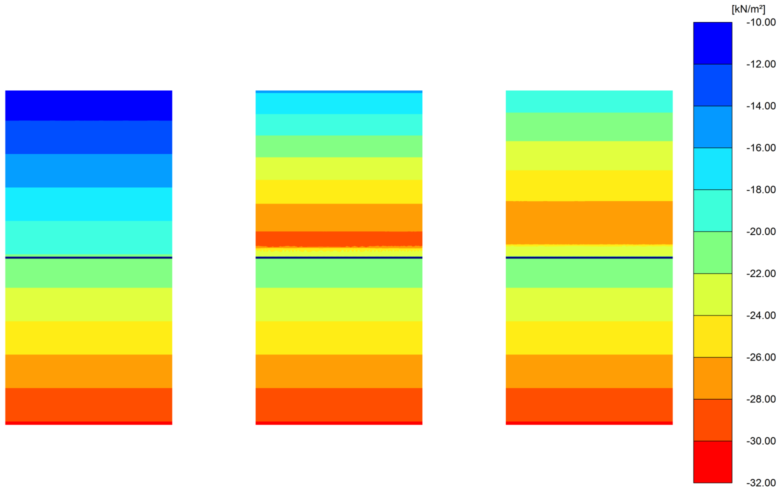


Figure 8 Vertical effective stresses after the plastic analysis (Phase 1) in PLAXIS 2D

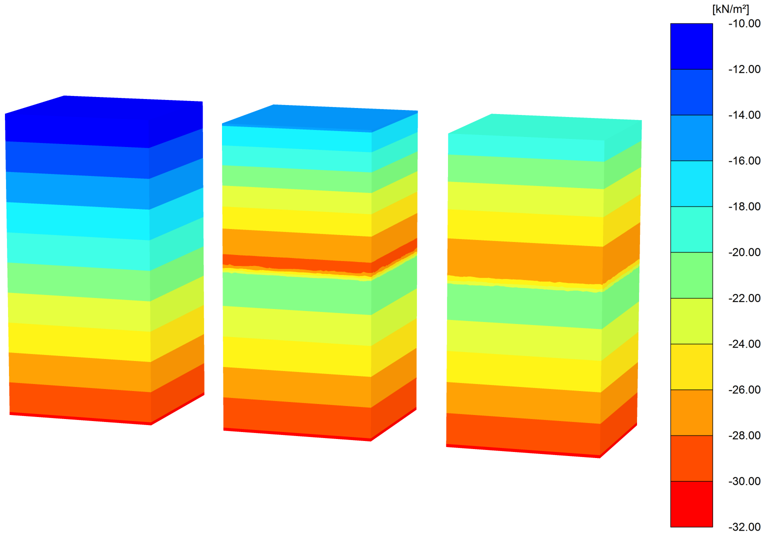


Figure 9 Vertical effective stresses after the plastic analysis (Phase 1) in PLAXIS 3D

$$K' = \frac{E'}{3(1-2\nu')} \quad (6)$$

Based on the input parameters used in the present example, $E^{sat}_{oed,u}$ = 50500 kPa. With respect to the unsaturated soil condition of cases 1 and 2 at the top of the model (suction equal to 10 kPa), $E^{unsat,coarse}_{oed,u}$ = 1007.59 kPa and $E^{unsat,fine}_{oed,u}$ = 1021.78 kPa.

The volumetric strain $\epsilon_v$ is obtained from the total vertical stress $\sigma_v$ as:

$$\epsilon_v = \frac{\sigma_v}{E_{oed,u}} \quad (7)$$

The water pore pressures $p_w$ is derived as:

$$p_w = p_{steady} + p_{excess} = p_{steady} + \epsilon_v \frac{K_w}{n} \tag{8}$$

in which $K_w$ is $K_w^{sat}$ for S = 1, $K_w^{unsat,coarse}$ for the coarse material with S < 1 and $K_w^{unsat,fine}$ for the fine material with S < 1.

Bishop's effective stress (Bishop & Blight, 1963) is given as:

$$\sigma' = \sigma - m \cdot [\chi p_w + (1 - \chi) p_\alpha] \tag{9}$$

in which,

$$\begin{aligned} \sigma &= \begin{bmatrix} \sigma_{xx} & \sigma_{yy} & \sigma_{zz} & \tau_{xy} & \tau_{yz} & \tau_{xz} \end{bmatrix}^T \\ \sigma' &= \begin{bmatrix} \sigma'_{xx} & \sigma'_{yy} & \sigma'_{zz} & \tau_{xy} & \tau_{yz} & \tau_{xz} \end{bmatrix}^T \\ m &= \begin{bmatrix} 1 & 1 & 1 & 0 & 0 & 0 \end{bmatrix}^T \end{aligned} \tag{10}$$

In Eq. (9), $\sigma$ is the vector of total stresses, $\sigma'$ is the vector of effective stresses, $p_\alpha$ is the pore air pressure and $\chi$ is the matric suction coefficient. In general, $\chi$ is determined experimentally, being a function of the degree of saturation, the porosity and the matric suction ($p_\alpha - p_w$) (Khalili & Khabbaz, 1998). Due to lack of experimental data, $\chi$ is often assumed equal to the effective saturation $S_{eff}$ (Bolzon, Schrefler & Zienkiewicz, 1996), which is given as:

$$S_{eff} = \frac{S - S_{res}}{S_{sat} - S_{res}} \tag{11}$$

All three cases presented above are studied analytically and the obtained results are compared with PLAXIS results in Table 2 for case 1, Table 3 for case 2 and Table 4 for case 3. The results at the top model boundary (unsaturated condition for cases 2 and 3) are presented. For both PLAXIS 2D and PLAXIS 3D results, a vertical cross-section at the middle of the model (x = 0.5 m) is considered.

The degree of saturation is degraded faster with increasing suction in coarse material (Figure 3), therefore less excess pore pressure is expected in the unsaturated zone (compare $p_{excess}^{top}$ in Table 3 and Table 4). In addition, the decrease in the degree of saturation is not linear, which results in non-linear distribution of effective stresses as well.

It is concluded that the undrained behaviour of soil is correctly implemented in PLAXIS.

Table 2 Comparison between analytical and PLAXIS results for fully saturated material (case 1, Phase 1, plastic analysis)

| Parameter | Result | | | Error | |
|---|---|---|---|---|---|
| | Analytical | PLAXIS 2D | PLAXIS 3D | PLAXIS 2D | PLAXIS 3D |
| $S$ (-) | 1.0 | 1.0 | 1.0 | 0.00 % | 0.00 % |
| $\epsilon_v^{top}$ (-) | $-0.198 \cdot 10^{-3}$ | $-0.198 \cdot 10^{-3}$ | $-0.198 \cdot 10^{-3}$ | 0.00 % | 0.00 % |
| $\sigma^{top}$ (kPa) | -10.0 | -10.0 | -10.0 | 0.00 % | 0.00 % |
| $p_{excess}^{top}$ (kPa) | -9.801 | -9.802 | -9.802 | 0.01 % | 0.01 % |
| $p_w^{top}$ (kPa) | 0.199 | 0.198 | 0.198 | 0.50 % | 0.50 % |
| $\sigma'^{top}$ (kPa) | -10.199 | -10.198 | -10.198 | 0.01 % | 0.01 % |

Table 3 Comparison between analytical and PLAXIS results for partially saturated *coarse* material (case 2, Phase 1, plastic analysis)

| Parameter | Result | | | Error | |
|---|---|---|---|---|---|
| | Analytical | PLAXIS 2D | PLAXIS 3D | PLAXIS 2D | PLAXIS 3D |
| $S$ (-) | 0.6049 | 0.6062 | 0.6062 | 0.00 % | 0.13 % |
| $\epsilon_v^{top}$ (-) | $-9.925 \cdot 10^{-3}$ | $-9.963 \cdot 10^{-3}$ | $-9.966 \cdot 10^{-3}$ | 0.38 % | 0.41 % |
| $\sigma^{top}$ (kPa) | -10.0 | -10.0 | -10.0 | 0.00 % | 0.00 % |
| $p_{excess}^{top}$ (kPa) | -0.075 | -0.076 | -0.076 | 1.33 % | 1.33 % |
| $p_w^{top}$ (kPa) | 9.925 | 9.924 | 9.924 | 0.01 % | 0.01 % |
| $\sigma'^{top}$ (kPa) | -15.744 | -15.751 | -15.76 | 0.04 % | 0.08 % |

Table 4 Comparison between analytical and PLAXIS results for partially saturated *fine* material (case 3, Phase 1, plastic analysis)

| Parameter | Result | | | Error | |
|---|---|---|---|---|---|
| | Analytical | PLAXIS 2D | PLAXIS 3D | PLAXIS 2D | PLAXIS 3D |
| $S$ (-) | 0.8623 | 0.8623 | 0.8638 | 0.00 % | 0.17 % |
| $\epsilon_v^{top}$ (-) | $-9.787 \cdot 10^{-3}$ | $-9.823 \cdot 10^{-3}$ | $-9.826 \cdot 10^{-3}$ | 0.37 % | 0.40 % |
| $\sigma^{top}$ (kPa) | -10.0 | -10.0 | -10.0 | 0.00 % | 0.00 % |
| $p_{excess}^{top}$ (kPa) | -0.213 | -0.215 | -0.215 | 0.94 % | 0.94 % |
| $p_w^{top}$ (kPa) | 9.787 | 9.785 | 9.785 | 0.02 % | 0.02 % |
| $\sigma'^{top}$ (kPa) | -18.413 | -18.419 | -18.42 | 0.03 % | 0.06 % |

## REFERENCES


[1] Bishop, A.W., Blight, G.E. (1963). Some aspects of effective stress in saturated and partly saturated soils. Géotechnique, 13(3), 177–197.

[2] Bishop, A.W., Eldin, G. (1950). Undrained triaxial tests on saturated sands and their significance in the general theory of shear strength. Géotechnique, 2(1), 13–32.

[3] Bolzon, G., Schrefler, B., Zienkiewicz, O. (1996). Elastoplastic soil constitutive laws generalized to partially saturated states. Géotechnique, 46(2), 279–289.

[4] Fredlund, D.G., Rahardjo, H. (1993). Soil mechanics for unsaturated soils. John Wiley & Sons.

[5] Khalili, N., Khabbaz, M. (1998). A unique relationship of $\chi$ for the determination of the shear strength of unsaturated soils. Géotechnique, 48(5), 681–687.

[6] van Genuchten, M.T. (1980). A closed-form equation for predicting the hydraulic conductivity of unsaturated soils. Soil science society of America journal, 44(5), 892–898.

[7] Verruijt, A. (2001). Soil mechanics. Delft University of Technology.